Agronomy Research **18**(S2), 1323–1335, 2020
https://doi.org/10.15159/AR.20.095

Modelling of hot-air and vacuum drying of persimmon fruit (*Diospyros kaki*) using computational intelligence methods

A.Y. Khaled[1,*], A. Kabutey[1], C. Mizera[1], P. Hrabe[2] and D. Herák[1]

[1]Department of Mechanical Engineering, Faculty of Engineering, Czech University of Life Sciences Prague, Kamýcká 129, CZ165 00 Praha-Suchdol, Czech Republic
[2]Department of Material Science and Manufacturing Technology, Faculty of Engineering, Czech University of Life Sciences Prague, Kamýcká 129, CZ165 00 Praha-Suchdol, Czech Republic
[*]Correspondence: f_yahya87@hotmail.com

Abstract. The study evaluated the feasibility of applying computational intelligence methods as a non-destructive technique in describing the drying behaviour of persimmon fruit using vacuum drying (VD) and hot-air-drying (HAD) methods and to compare the results with thin layer mathematical models. Drying temperatures were 50, 60 and 70 °C. Kinetic models were developed using semi-theoretical thin layer models and computational intelligence methods: multi-layer feed-forward artificial neural network (ANN) and support vector regression (SVR). The statistical indicators of coefficient of determination (R^2) and root mean square error (RMSE) were used to assess the suitability of the models. The thin-layer mathematical models namely page and logarithmic accurately described the drying kinetics of persimmon slices with the highest R^2 of 0.9999 and lowest RMSE of 0.0031. ANN showed R^2 and RMSE values of 1.0000 and 0.0003, while SVR showed R^2 of 0.9999 and RMSE of 0.0004. The validation results indicated good agreement between the predicted values obtained from the computational intelligence methods and the experimental moisture ratio data. Based on the study results, computational intelligence methods can reliably be used to describe the drying process of persimmon fruit.

Key words: persimmon fruit, drying methods, computational intelligence methods, artificial neural network model, support vector regression model.

INTRODUCTION

Persimmon (*Diospyros kaki*) is an edible fruit that grows in subtropical and warm temperate climates and it is considered an important fruit in many countries such as China, Japan and Korea and Turkey. It has a high nutritional value such as vitamin A, C, carotenoid and phenolic compounds (Bozkir et al., 2019). The high moisture content of the fruit leads to rapid deterioration even at refrigerator temperatures. Therefore, drying is considered as one of the processes to increase persimmon shelf life. This indicates that persimmon can be used as an ingredient in products such as breakfast cereals and snacks (Doymaz, 2012).

Drying of agricultural products causes the enzymatic reactions to be inactivated as a result of heat and mass transfer leading to a reduction of the moisture content inside the product (Tomsone et al., 2018). Drying methods such as hot-air drying (HAD),

freeze-drying (FD), vacuum drying (VD), microwave drying (MWD) and infrared drying (IRD) have been used in drying agricultural products (Doymaz, 2012; Karaman et al., 2014). However, HAD is the most commonly used technique due to the uniformity of the dried product and non-toxicity (Onwude et al., 2016b; Ozola & Kampuse, 2018). In the VD method, the use of low temperatures in the absence of oxygen can preserve heat-sensitive and easily oxidizable foods where discoloration and decomposition of the flavor and some nutritional substances are prevented (Tekin & Baslar, 2018; Karasu et al., 2019). Both HAD and VD can also affect the physical and phytochemical properties of the food products. Hence, the determination of the optimum operating parameters, drying conditions and the determination of suitable drying models are important for achieving the nutritional value along with minimum product cost and maximum yield (Tomsone et al., 2018).

Some studies have explored several thin-layer drying models to describe the drying processes of fruits and vegetables. The thin-layer drying models are empirical, semi-theoretical and theoretical models based on the assumption of mass diffusivity, conductivity and geometry (Akoy, 2014; Aboltins et al., 2018). Theoretical models have followed the fundamentals of mass and heat transfer laws during the drying process and their parameters have a physical meaning (Górnicki et al., 2020). In practical, according to (Kaleta & Górnicki, 2010) theoretical models normally take a long time due to the complexity of the diffusion equations governing the process. Semi-theoretical models offer a compromise between theory and ease of application and they are deduced from simplified versions of Fick's second law of diffusion (Ashtiani et al., 2017). Empirical models are basically built between the direct relationship between the curve of moisture content and drying time and does not need to consider the theory during the drying process (Kaleta et al., 2013). These models, however, do not produce accurate results (Onwude et al., 2016b). Thus, researchers are considering new drying modelling approaches or computational tools.

Computational tools such as artificial neural networks (ANN) and support vector regression (SVR) are considered as complex tools for complex systems and dynamic modelling (Khaled et al., 2018). Application of ANN and SVR offer many advantages compared to conventional modeling techniques due to the learning ability, increased flexibility, online non-destructive measurements, reduced assumptions, suitability to the nonlinear process and tolerance of incomplete data (Rodríguez et al., 2014). The difference between ANN and SVR is fundamentally based on how the non-linear data is classified. For example, ANN applies a multi-layer connection and different activation functions to deal with nonlinear problems. While SVM employs nonlinear mapping to make the data linear separable using kernel functions (Khaled et al., 2020).

ANN and SVR have been successfully applied in modelling and optimizing the drying processes of fruits and vegetables such as pomelo (Kırbaş et al., 2019), ginkgo biloba seeds (Bai et al., 2018), mushroom (Omari et al., 2018), celeriac slices (Beigi & Ahmadi, 2018), pepper (Jafari et al., 2016), eggplant (Bahmani et al., 2016), tea leaves (Xie et al., 2014), tomato (Movagharnejad & Nikzad, 2007). In view of this, ANN and SVR techniques can be applied to the drying kinetics of persimmon fruit under HAD and VD, and this knowledge is limited in the literature. This modelling technique can also be useful for assessing the drying parameters in real conditions, optimum processing conditions and drying efficiency.

The objectives of this study are to evaluate the feasibility of applying ANN and SVR modelling as a non-destructive technique in describing the drying behaviour of persimmon fruit under different drying conditions and to compare the results with thin layer mathematical models. Also, to investigate the color change kinetics of persimmon slices under different drying conditions during the VD and HAD.

MATERIALS AND METHODS

Samples preparation and moisture content determination

Persimmon fruits (*Diospyros kaki*) bought from a market in Prague, Czech Republic, were used for the experiment. A total of 30 samples were selected based on similar physical appearances (shape color and size). Prior to each experiment, the samples were peeled and washed under running tap water. Then they were sliced into thickness and diameter of 5 mm and 56 mm, respectively, using a Sencor slicer (SFS 4050SS, Czech Republic). The persimmon fruit with a sliced section of dimension 56 mm and thickness of 5 mm used in the study is shown in Fig. 1. The initial moisture content of the fresh samples was determined as 3.98 kg kg^{-1} (dry basis), according to ASABE standard (ASAE, 2005), by drying 25 g of selected samples at 70 °C for 24 h using the conventional oven.

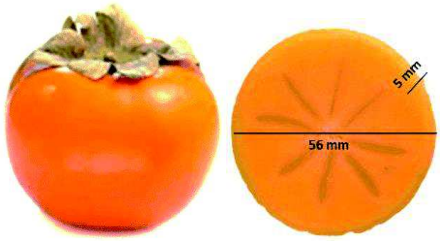

Figure 1. Persimmon fruit with a sliced section of diameter 56 mm and thickness of 5 mm.

Drying experiments

In this study, two different drying processes were used include VD and HAD to dry the persimmon sliced samples.

Vacuum drying

The VD technique was carried out using a laboratory-scale drying unit (l 450 Goldbrunn, Poland) as shown in Fig. 2. For VD, the vacuum was regulated by a vacuum pump (VE 135, RoHS, China) at a 50 mbar ultimate pressure and 2 Ls^{-1} pump speed. It is worth noting that the pressure was monitored through the vacuum gauge which was unstable during the drying process. This problem was solved manually by fixing the pressure at approximately 50 mbar. This meant that when the

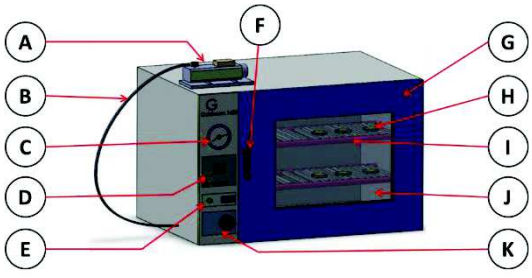

Figure 2. Schematic diagram of the vacuum dryer; A: vacuum pump; B: pipe; C: vacuum gauge; D: temperature regulator; E: ON/OFF master switch; F: door handle; G: door; H: sample; I: shelves; J: inspection window and K: vacuum valve.

pressure increased above or decreased below 50 mbar, the pump was opened for the adjustment. The VD operates by heating the samples with a conduction heat from a heater plate in the container. The vacuum pump reduces the pressure around the sample to be dried and further ensures less atmospheric pressure. This decreases the boiling point of the water inside that product and thereby increases the rate of evaporation significantly. The sliced samples were dried at three temperatures (50 °C, 60 °C, and 70 °C). Prior to the experiments, the VD was set-up to the required temperature for 30 min to enable the dryer temperature to reach equilibrium with the surrounding air temperature. The weight of the persimmon sample was measured 1 hour interval using a digital scale (HR-250AZ, A&D Company Limited) weighing balance of 252 g 0.1 mg^{-1} precision. The weight of the samples was measured during the drying process every 1 hour. The experiments were carried out in triplicate and the average values used in further analyses.

Hot-air drying

A laboratory-scale convective HAD (UF 110, Memmert, Germany) was used. Similar to VD, three temperatures (50 °C, 60 °C, and 70 °C) with a constant air velocity of 1.10 ms^{-1}, until constant weight between two successive readings was attained. The air velocity was measured using a Thermo–Anemometer (Model 451104, EXTECH Instruments, Taiwan). Before starting the experiments, the HAD was set-up to the required temperature for 30 min to enable the dryer temperature to reach equilibrium with the surrounding air temperature. Similar to the VD, the weight of the persimmon sample was measured 1 hour interval using a digital scale weighing balance, whereby the samples were removed from the dryer and measured and then returned to the dryer. The mass interval was expressed as the moisture ratio as illustrated in Fig. 4. The experiments were conducted in triplicate and the average values used in further analyses.

Drying kinetics

The variation in moisture content during VD and HAD techniques was expressed in the form of moisture ratio (dimensionless) as described in Eq. 1.

$$MR = \frac{(M_t - M_e)}{(M_o - M_e)} \quad (1)$$

where M_t, M_e and M_o are the moisture content of the samples at time t, equilibrium moisture content and initial moisture content, respectively.

According to Aghbashlo et al. (2009), M_e values did not change because they were relatively low compared to M_t and M_o values, resulting in negligible error during simplification, thus the moisture ratio was expressed as shown in Eq. 2:

$$MR = \frac{M_t}{M_o} \quad (2)$$

Mathematical modelling

The experimental drying data measured were fitted to 5 selected thin-layer drying models. The selected mathematical models, namely, Newton, Page, Logarithmic, Two-term and Modified Henderson and Pabis as listed in Table 1 using the non–linear least squares regression analysis using Sigma Plot software (Version 12.0, Systat Software Inc., California, USA). The use of these models gives a better prediction with fewer assumptions (Onwude et al., 2018).

Table 1. Thin layer mathematical drying models

Model no.	Model name	Model expression	Reference
1.	Newton model	MR = exp(-*kt*)	(Lewis, 1921)
2.	Page model	MR = exp(-kt^n)	(Page, 1949)
3.	Logarithmic model	MR= aexp(-*kt*)+*c*	(Yagcioglu, 1999)
4.	Two-term model	MR=*a*exp(-k_1t)+*b*exp(-k_2t)	(Henderson, 1974)
5.	Modified Henderson and Pabis model	MR=*a*exp(-*kt*)+*b*exp(-*gt*)+*c*exp(-*ht*)	(Karathanos, 1999)

Computational intelligence methods

Artificial neural network

Artificial Neural Network (ANN) is a powerful and complex modelling tool for processing model information based on biological neural networks (Khaled et al., 2018). In general, ANNs are created with three layers (input, hidden and output layer). In this study, a multilayer feed-forward network structure was used with three input parameters (drying techniques, temperature and drying time), 1–2 hidden layers and one output parameter (moisture ratio) as shown in Fig. 3. Algorithms applied to the training of the model were the Levenberg-Marquardt back propagation transfer function choice and sigmoid function as given in Eq. 3.

$$f(x) = \frac{1}{1 + e^{-x}} \tag{3}$$

The datasets were prepared by randomly dividing the data into training (70%) and testing (30%). The total number of data used in this study was 137 with 96 was used to build the model and 41 was used for testing the model. The chosen hidden layer architectures were [3], [6], [3, 3], [6, 6] matrix, where for example, [3, 3] represents the 2 hidden layers with 6 neurons (Fig. 3). The software Weka 3.6 (Hamilton, New Zealand) was used to analyse the ANN model. In this study, the error was used as the criteria to stop training to prevent the overtraining of ANN structure. This means that when the error against the iterations shows no change and it's saturated, then the ANN training is stopped.

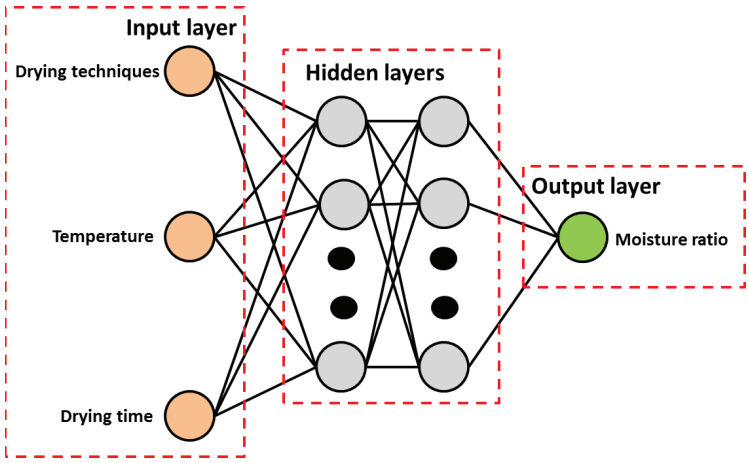

Figure 3. Artificial Neural networks topology.

Support vector regression

Support Vector Regression (SVR) is a supervised learning model which combines theoretical solutions with numerical algorithms used for regression method (Das & Akpinar, 2018). SVR as a regression method is considered as an effective approach due to its capability of capturing nonlinear relationship in the feature space. The SVR used for the moisture ratio values was determined by the SMOreg sequence in the Waikato Environment for Knowledge Analysis (WEKA) software, whereby, the SMOreg implements SVR for regression. The three input variables used for the SVR model were drying techniques, temperature and drying time with the output as the moisture ratio. In addition, two filter types were applied, namely normalize and standardize in order to determine how/if the data need to be transformed. Furthermore, three different kernel models: polynomial, Pearson universal and Radial Basis Function (RBF) were used to construct the predictive model of the calculated moisture ratio values.

Color measurements

Color is one of the most important quality evaluation attributes for fruits and vegetables during drying. For the color measurements, first the image of fresh (reference) and dried samples obtained from VD and HAD methods were captured using smartphone camera (Oppo F7, Dongguan, China). The smartphone camera consisted of a 16 mega-pixel charged-coupled device (CCD). Persimmon slices were put in a glass plate located on the white paper as a background during image capture for more focus, and the distance between sample and smartphone camera was set-up to be 22 cm vertically. Then the images were transferred to ImageJ software, which is an open-source software available to the public domain (http://rsb.info.nih.gov/ij/). Also, it can operate on Linux, Mac OS X, and Windows, in both 32-bit and 64-bit modes. ImageJ has different tools to analyse the images. In this study, ImageJ was used to determine the color parameters: lightness (L^*), redness/greenness (a^*) and yellowness/blueness (b^*). The total color difference (ΔE) was estimated based on Eq. 4. For each sample, three replications were performed.

$$\Delta E = \sqrt{(L^* - L_o^*)^2 + (a^* - a_o^*)^2 + (b^* - b_o^*)^2} \quad (4)$$

where L_o^*, a_o^* and b_o^* indicate the reference values of fresh samples.

Statistical analysis for mean comparison

Statistical analysis was performed using the Statistical Analysis System software (SAS version 9.2, Institute, Inc., Cary, N.C.). Duncan test was used to compare the mean significant differences between quality attributes (L^*, a^*, b^* and ΔE) for different drying time intervals and at different drying techniques (VD and HAD). The findings of replicate measurements were presented with mean ± standard error values. The fit accuracy of experimental data to the thin layer, ANN and SVR models was determined by the coefficient of determination (R^2) and root mean square error (RMSE). They are computed mathematically as given in Eqs 5 and 6:

$$R^2 = 1 - \frac{\sum_{i=1}^{N}(V_{pred} - V_{exp})^2}{\sum_{i=1}^{N}(V_{pred} - V_m)^2} \quad (5)$$

$$RMSE = \sqrt{\frac{\sum_{i=1}^{N}(V_{pred} - V_{exp})^2}{N}} \quad (6)$$

where V_{pred} is the predicted value, V_{exp} is the actual observation from experimental data, V_m is the mean of the actual observation, and N is number of observations.

From the values of R^2 and RMSE, the higher the value of R^2 and the lower the RMSE value, the better the goodness of fit.

RESULTS AND DISCUSSION

Behaviour of drying process of persimmon fruit slices

The variations of moisture ratio with time for VD and HAD techniques at different temperatures (50 °C, 60 °C, and 70 °C) are illustrated in Fig. 4. The moisture ratio of the samples for all techniques decreased with an increase in drying time. The drying rates for VD and HAD methods occurred in the falling rate period. Based on Fig. 4, a, it is clear that the drying time thus reduces as the drying temperature increases. The moisture ratio values of 0.18 and 0.22 were determined at a drying time of 170 min and at temperatures of 70 °C and 60 °C. At a drying time of 360 min was found the moisture ratio of 0.22 at 50 °C. Similar results were observed using HAD (Fig. 4, b). The results indicate that the moisture transfer rate from the inner layers to its surface thus increases as the drying air temperature increases. The rate of moisture evaporation at the surface of the persimmon sample to the atmosphere also increases as the temperature increases, leading to the higher drying rate. For this, the drying time for persimmon samples using HAD was different from VD. The results are in agreement with other researchers on the drying behaviour of various varieties of persimmon (Çalışkan & Dirim, 2015; Bozkir et al., 2019).

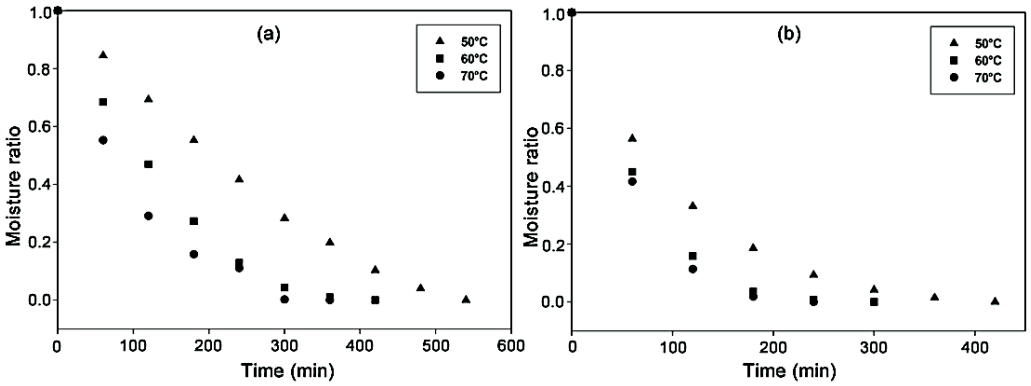

Figure 4. Drying characteristics of persimmon fruit sliced samples; [a] VD and [b] HAD.

Comparison between the mathematical modelling

The mathematical models were applied to describe the drying kinetic of persimmon slices during VD and HAR methods. Table 2 shows the selected mathematical models that fitted the experimental moisture content data. Although all the selected five models adequately fitted the experimental data, the logarithmic model sufficiently described the drying kinetics of the samples with R^2 values between 0.9964 and 0.9980 and RMSE values between 0.0146 and 0.0206 for VD technique at all drying temperatures. For HAD technique, Page and logarithmic models significantly described the drying kinetics of the samples with R^2 values between 0.9979 and 0.9999 RMSE values between 0.0031

and 0.0171. The validation of the logarithmic model by comparing the predicted moisture data and those obtained from the experiments is presented in Fig. 5. The moisture ratio data predicted using logarithmic model lied closely along a straight regression line for different drying conditions indicating the suitability of the model for describing the VD and HAD behaviours of persimmon fruit samples. Onwude et al., (2018) also reported the adequacy of Page and logarithmic models for predicting the drying kinetics of sweet potato. Similarly, Younis et al. (2018) indicated the appropriateness of page and logarithmic models for describing the drying performance of garlic slices.

Table 2. Statistical evaluation of the mathematical drying models for persimmon samples of VD and HAD

Drying method	Temp °C	Model no	Model parameters	R^2	RMSE
VD	50	1	k = 0.2491	0.9577	0.0682
		2	k = 0.1224, n = 1.4734	0.9940	0.2559
		3	a = 1.5532, k = 0.1229, c = -0.5369	0.9980	0.0146
		4	a = 0.5606, k_1 = 0.2663, b = 0.5108, k_2 = 0.2663	0.9650	0.0620
		5	a = 0.3715, k = 0.2663, b = 0.3610, g = 0.2663, c = 0.3388, h = 0.2663	0.9650	0.0620
	60	1	k = 0.4503	0.9821	0.0457
		2	k = 0.3292, n = 1.3069	0.9960	0.0217
		3	a = 1.1435, k = 0.3445, c = -0.1331	0.9964	0.0206
		4	a = 0.5347, k_1 = 0.4632, b = 0.4988, k_2 = 0.4632	0.9836	0.0438
		5	a = 0.3531, k = 0.4632, b = 0.3503, g = 0.4632, c = 0.3300, h = 0.4632	0.9836	0.0438
	70	1	k = 0.6145	0.9957	0.0220
		2	k = 0.5871, n = 1.0608	0.9963	0.0205
		3	a = 1.0325, k = 0.5613, c = -0.0345	0.9974	0.0173
		4	a = 0.5045, k_1 = 0.6171, b = 0.5003, k_2 = 0.6171	0.9958	0.0219
		5	a = 0.3329, k = 0.6171, b = 0.3408, g = 0.6171, c = 0.3312, h = 0.6171	0.9958	0.0219
HAD	50	1	k = 0.5737	0.9986	0.0120
		2	k = 0.5514, n = 1.0481	0.9990	0.0103
		3	a = 1.0228, k = 0.5349, c = -0.0255	0.9998	0.0047
		4	a = 0.5027, k_1 = 0.5753, b = 0.5005, k_2 = 0.5753	0.9987	0.0120
		5	a = 0.3315, k = 0.5753, b = 0.3405, g = 0.5753, c = 0.3313, h = 0.5753	0.9987	0.0120
	60	1	k = 0.8838	0.9957	0.0235
		2	k = 0.7945, n = 1.2519	0.9998	0.0047
		3	a = 1.0409, k = 0.8064, c = -0.0359	0.9982	0.0152
		4	a = 0.5142, k_1 = 0.8898, b = 0.4950, k_2 = 0.8898	0.9958	0.0232
		5	a = 0.3401, k = 0.8898, b = 0.3409, g = 0.8898, c = 0.3282, h = 0.8898	0.9958	0.0232
	70	1	k = 0.9781	0.9943	0.0284
		2	k = 0.8745, n = 1.3348	0.9999	0.0031
		3	a = 1.0564, k = 0.8581, c = -0.0522	0.9979	0.0171
		4	a = 0.5158, k_1 = 0.9840, b = 0.4928, k_2 = 0.9840	0.9944	0.0281
		5	a = 0.3409, k = 0.9840, b = 0.3408, g = 0.9840, c = 0.3270, h = 0.9840	0.9944	0.0281

Temp: Temperature.

Artificial neural network (ANN)

Time, temperature and drying techniques were used to predict moisture ratio using ANN model. Table 3 shows the statistical results related to the training and validation of the multilayer feed-forward network structure of experimental data. The training data set were used to assess the optimum number of neurons and hidden layers for multilayer neural network modelling for determining the best predictive power. The results illustrated that the architecture with 2 hidden layers and 6 neurons [3, 3], obtained the best results as compared to those of 1 hidden layer [3, 6 and 9 neurons] and 2 hidden layers (12 and 18 neurons), respectively. Moreover, the networks were found to be susceptible to the number of neurons in their hidden layers. Thus, smaller neurons led to under-fitting, while too many neurons contributed to overfitting. From the results produced from ANN model, the highest R^2 and the lowest RMSE values of 1.0000 and 0.0003, respectively as listed in Table 3. These results indicated that ANN found higher results compared to page model (R^2 = 0.9999 and RMSE = 0.0031) as shown in Table 2. Zenoozian et al. (2014) found that 2 hidden layers and 30 neurons adequately predicted the moisture changes during the drying kinetics of pumpkin. ANN with 2 hidden layers has also been successful in predicting the drying behaviour of other fruits and vegetables such as pumpkin, pepper, apple slices during microwave-vacuum drying (Nadian et al., 2014; Jafari et al., 2016; Onwude et al., 2016a).

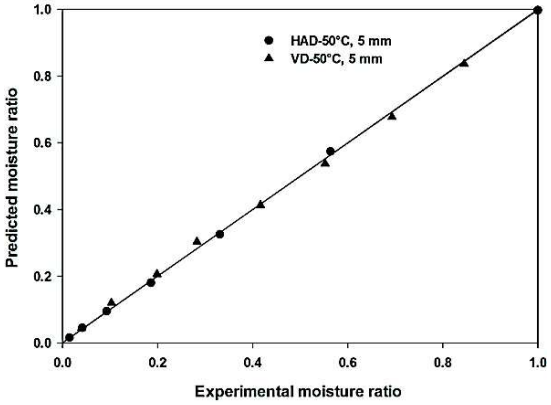

Figure 5. Predicted versus experimental moisture ratio data for logarithmic model at 50 °C for VD and HAD methods.

Table 3. ANN model statistical evaluation

No. hidden layer	No. Neurons	Training		Testing	
		R^2	RMSE	R^2	RMSE
1	3	0.9982	0.0167	0.9966	0.0290
1	6	0.9992	0.0038	0.9879	0.0363
1	9	0.9986	0.0209	0.9876	0.0819
2	**3.3**	1.0000	0.0003	0.9978	0.0089
2	6.6	0.9999	0.0013	0.9969	0.0275
2	9.9	0.9996	0.0019	0.9988	0.0269

Support vector regression (SVR)

The statistical results related to the training and validation of the SVR of persimmon drying experimental data are given in Table 4. Similar to ANN model, the training data set was used to evaluate the best filter and kernel type modelling for determining the best predictive power. The results showed that the normalize and standardize filter types with pearson universal kernel obtained the best results as compared to those of normalize with polynomial and RBF kernel and also standardize with polynomial, and RBF kernel, respectively. From the results of Table 2 and Table 4, it is clear that the SVR model produced the same value of R^2 (0.9999) as compared to the highest values of theoretical

mathematical models. However, the SVR model found the lowest RMSE of 0.0013 as compared to the lowest value of RMSE (0.0031) using page model from the theoretical mathematical models. Few studies used SVR as a model in drying techniques. Das & Akpinar, (2018) applied SVR to investigate pear drying performance by different ways of convective heat transfer. The authors applied normalization and standardization filter to the target attribute with three kernel models namely polynomial kernel, pearson universal kernel and RBF kernel. They found that polynomial kernel found the lowest RMSE of 0.3351. Generally, more efficient results for computational intelligence methods can be obtained when the parameters of ANN and SVR are optimized (Khaled et al., 2018).

Table 4. Statistical results for SVR model

Filter type	Kernel type	Training		Testing	
		R^2	RMSE	R^2	RMSE
Normalize	Polynomial kernel	0.9080	0.1538	0.8718	0.1601
Normalize	**Pearson universal kernel**	**0.9999**	0.0013	0.9303	0.1197
Normalize	RBF kernel	0.9976	0.0262	0.9364	0.2056
Standardize	Polynomial kernel	0.9728	0.0780	0.8717	0.1604
Standardize	**Pearson universal kernel**	**0.9999**	0.0004	0.9361	0.1094
Standardize	RBF kernel	0.9973	0.0271	0.9360	0.1098

Color measurements

The quality properties of persimmon fruit slices during VD and HAD methods were determined based on the change in color parameters of L^*, a^*, and b^* and the total color change ΔE as given in Table 5. It can be seen clearly from Table 5 that that the lightness (L^*) of the samples using VD and HAD methods decreased significantly ($p \leq 0.05$) compared to the fresh samples. However, there was no significant difference between the lightness of samples using VD at 60 °C and 70 °C and also HAD from 50 to 70 °C for fresh samples. Lightness of samples using VD at 50 °C was significantly different compared to the fresh samples. Using VD significantly ($p \leq 0.05$) reduced the lightness of samples compared to HAD. VD at 50 °C showed the lowest lightness values of 52.560 ± 3.680. The redness/greenness (a^*) of samples reduced significantly ($p \leq 0.05$) compared to fresh samples. There was no significant difference between the redness/greenness of samples using VD at 50 °C and HAD at 50 °C in comparison with fresh samples. Generally, the values of redness/greenness (a^*) using HAD were higher than VD, except the value using VD at 60 °C. The lowest value of redness/greenness (a^*) was 11.684 ± 0.259 using HAD at 60 °C. Similar results were found for the yellowness/blueness (b^*), where the color of all dried samples reduced significantly ($p \leq 0.05$) compared to the fresh samples. In addition, there was no significant difference between the b^* of fresh samples with those of dried samples using VD at 60 °C and 70 °C, and HAD from 50 to 70 °C respectively. Dried samples using VD at 50 °C showed yellowness/blueness mean value of 56.040 ± 3.410. The values of total color change using the VD method were higher compared to the HAD method. The highest value of 17.790 ± 4.100 was found for VD at 50 °C. This could be due to the mechanisms involved in VD which thus gradually sucks the air compared to HAD. Generally, the change of color properties of the fresh samples under different drying methods is due to the increased sample

temperature resulting in increased enzymatic and non-enzymatic chemical reactions of the product (Nozad et al., 2016).

Table 5. Drying methods and color parameters of persimmon fruit.

Drying method	Temp ˚C	Color properties for different sample thickness			
		L*	a*	b*	ΔE
	Fresh	61.425 ± 2.533^{a}	26.282 ± 0.747^{a}	65.698 ± 2.126^{a}	-
VD	50	52.560 ± 3.680^{b}	$20.69 \pm 1.95bc^{ab}$	56.040 ± 3.410^{b}	17.790 ± 4.100^{a}
	60	56.161 ± 3.476^{ab}	16.280 ± 3.598^{bc}	61.073 ± 2.834^{ab}	15.859 ± 1.822^{ab}
	70	59.646 ± 0.413^{ab}	12.804 ± 0.764^{c}	62.265 ± 0.076^{ab}	14.568 ± 0.669^{ab}
HAD	50	56.930 ± 1.152^{ab}	23.438 ± 0.258^{a}	61.762 ± 1.088^{ab}	9.528 ± 1.568^{b}
	60	60.250 ± 2.229^{a}	11.684 ± 0.259^{c}	64.831 ± 2.231^{a}	14.928 ± 0.680^{ab}
	70	59.846 ± 1.149^{ab}	17.259 ± 1.164^{bc}	64.491 ± 0.750^{a}	10.140 ± 0.405^{b}

Temp: Temperature. Data represents the mean and three replicates (±standard error). Different letters at the same column indicates statistical difference for Duncan test, $p < 0.05$ for drying temperature.

CONCLUSIONS

The study investigated the potential of using computational intelligence as a modelling tool for predicting the drying process of persimmon fruit slices (samples). The results showed that VD and HAD had a significant effect on the drying kinetics and color properties of samples. As increase in drying temperature influenced the drying kinetics using HAD and VD. Dried samples using HAD showed significant color attributes compared to VD. The thin-layer modelling results showed that Page and logarithmic model can adequately ($R^2 = 0.9999$) described the drying kinetics of samples. Accurate results were found using ANN ($R^2 = 1.0000$) model. Computational intelligence methods and theoretical models gave similar results. However, the ANN and SVR models are able to describe a wider range of experimental data whereas the application of theoretical models is limited to specific experimental conditions in most cases. Thus, the ANN and SVR models may be considered as suitable alternative modelling methods for describing the drying behaviour of samples. On the other hand, computational intelligence methods can be successfully applied to industrial drying processes and operations as well as online monitoring and control.

ACKNOWLEDGEMENTS. The authors gratefully appreciate Czech University of Life Sciences Prague for the financial support provided under research grant (CZ.02.2.69/0.0/0.0/16_027/0008366).

REFERENCES

Aboltins, A., Rubina, T. & Palabinskis, J. 2018. Shrinkage effect on diffusion coefficient during carrot drying. *Agronomy Reseach* **16**(S2), 1301–1311.

Aghbashlo, M., Kianmehr, M.H., Khani, S., Ghasemi, M. & others. 2009. Mathematical modelling of thin-layer drying of carrot. *International Agrophysics* **23**(4), 313–317.

Akoy, E.O.M. 2014. Experimental characterization and modeling of thin-layer drying of mango slices. *International Food Research Journal* **21**(5).

ASAE. 2005. Moisture measurement – unground grain and seeds. *American Society of Agricultural and Biological Engineers* 2–4.

Ashtiani, S.M., Salarikia, A. & Golzarian, M.R. 2017. Analyzing drying characteristics and modeling of thin layers of peppermint leaves under hot-air and infrared treatments. *Information Processing in Agriculture* **4**(2), 128–139.

Bahmani, A., Jafari, S.M., Shahidi, S.-A. & Dehnad, D. 2016. Mass transfer kinetics of eggplant during osmotic dehydration by neural networks. *Journal of Food Processing and Preservation* **40(**5), 815–827.

Bai, J., Xiao, H., Ma, H. & Zhou, C. 2018. Artificial neural network modeling of drying kinetics and color changes of ginkgo biloba seeds during microwave drying process. *Journal of Food Quality* **2018**, 1–9.

Beigi, M. & Ahmadi, I. 2018. Artificial neural networks modeling of kinetic curves of celeriac (Apium graveolens L) in vacuum drying. *Food Science and Technology* **2061**, 1–6.

Bozkir, H., Rayman, A., Serdar, E., Metin, G. & Baysal, T. 2019. Ultrasonics - sonochemistry influence of ultrasound and osmotic dehydration pretreatments on drying and quality properties of persimmon fruit. *Ultrasonics - Sonochemistry 54*(December 2018), 135–141.

Çalışkan, G. & Nur Dirim, E. 2015. Freeze drying kinetics of persimmon puree. *GIDA*, **40**(1), 9–14.

Das, M. & Akpinar, E.K. 2018. Investigation of pear drying performance by different methods and regression of convective heat transfer coefficient with support vector machine. *Applied Sciences* **8**, 2–16.

Doymaz, I. 2012. Evaluation of some thin-layer drying models of persimmon slices (*Diospyros kaki L*). *Energy Conversion & Management* **56**, 199–205.

Górnicki, K., Kaleta, A. & Choińska, A. 2020. Suitable model for thin-layer drying of root vegetables and onion. *International Agrophysics* **34**(1), 79–86.

Henderson, S.M. 1974. Progress in developing the thin layer drying equation. *Transactions of the ASAE* **17**(6), 1167–1168.

Jafari, S.M., Ghanbari, V., Ganje, M. & Dehnad, D. 2016. Modeling the drying kinetics of green bell pepper in a heat pump assisted fluidized bed dryer. *Journal of Food Quality* **39**, 98–108.

Kaleta, A. & Górnicki, K. 2010. Some remarks on evaluation of drying models of red beet particles. *Energy Conversion and Management* **51**(12), 2967–2978.

Kaleta, A., Górnicki, K., Winiczenko, R. & Chojnacka, A. 2013. Evaluation of drying models of apple (var. Ligol) dried in a fluidized bed dryer. *Energy Conversion and Management* **67**, 179–185.

Karaman, S., Toker, O.S., Çam, M., Hayta, M., Kayacier, A., Karaman, S., … Kayacier, A. 2014. Bioactive and physicochemical properties of persimmon as affected by drying methods. *Drying Technology* **32**, 258–267.

Karasu, S., Akcicek, A. & Kayacan, S. 2019. Effects of different drying methods on drying kinetics, microstructure, color, and the rehydration ratio of minced meat. *Foods* **8**, 2–14.

Karathanos, V.T. 1999. Determination of water content of dried fruits by drying kinetics. *Journal of Food Engineering* **39**(4), 337–344.

Khaled, A.Y., Aziz, S.A., Bejo, S.K., Nawi, N.M., Jamaludin, D., Ul, N. & Ibrahim, A. 2020. A comparative study on dimensionality reduction of dielectric spectral data for the classi fi cation of basal stem rot (BSR) disease in oil palm. *Computers and Electronics in Agriculture* **170**, 105288.

Khaled, A.Y., Aziz, S.A., Bejo, S.K., Nawi, N.M. & Seman, I.A. 2018. Spectral features selection and classification of oil palm leaves infected by Basal stem rot (BSR) disease using dielectric spectroscopy. *Computer and Electronics in Agriculture* **144**, 297–309.

Kırbaş, İ., Doğuş, A., Şirin, C. & Usta, H. 2019. Modeling and developing a smart interface for various drying methods of pomelo fruit (Citrus maxima) peel using machine learning approaches. *Computer and Electronics in Agriculture* **165**(June), 2–8.

Lewis, W. 1921. The rate of drying of solid materials. *The Journal of Industrial and Engineering Chemistry 13*(5), 427–432.

Movagharnejad, K. & Nikzad, M. 2007. Modeling of tomato drying using artificial neural network. *Computer and Electronics in Agriculture* **59**, 78–85.

Nadian, M.H., Rafiee, S., Aghbashlo, M., Hosseinpour, S. & Mohtasebi, S.S. 2014. Continuous real-time monitoring and neural network modelling of apple slices color changes during hot air Drying. *Food and Bioproducts Processing*, pp. 1–40.

Nozad, M., Khojastehpour, M. & Tabasizadeh, M. 2016. Characterization of hot-air drying and infrared drying of spearmint (Mentha spicata L) leaves. *Journal of Food Measurement and Characterization* **10**, 466–473.

Omari, A., Behroozi-Khazaei, N. & Sharifian, F. 2018. Drying kinetic and artificial neural network modeling of mushroom drying process in microwave-hot air dryer. *Food Process Engineering* **41**(7), 1–10.

Onwude, D.I., Hashim, N., Abdan, K., Janius, R. & Chen, G. 2018. Modelling the mid-infrared drying of sweet potato : kinetics, mass and heat transfer parameters, and energy consumption. *Heat and Mass Transfer* **54**, 2917–2933.

Onwude, D.I., Hashim, N., Janius, R.B., Nawi, N. & Abdan, K. 2016a. Modelling the convective drying process of pumpkin (Cucurbita moschata) using an artificial neural network. *International Food Research Journal* **23**(Suppl), S237–S243.

Onwude, D.I., Hashim, N., Janius, R.B., Nawi, N.M. & Abdan, K. 2016b. Modeling the thin-layer drying of fruits and vegetables: A review. *Comprehensive Reviews in Food Science and Food Safety* **15**(3), 599–618.

Ozola, L. & Kampuse, S. 2018. The influence of drying method to the changes of bioactive compounds in lingonberry by-products. *Agronomy Reseach* **16**(4), 1781–1795.

Page, G. 1949. *Factors influencing the maximum rates of air drying shelled corn in thin layers*. Purdue University, ProQuest Dissertations Publ., West Latayette, IN, USA.

Rodríguez, J., Clemente, G., Sanjuán, N. & Bon, J. 2014. Modelling drying kinetics of thyme (Thymus vulgaris L.): Theoretical and empirical models, and neural networks. *Food Science and Technology International* **20**(1), 13–22.

Tekin, Z.H. & Baslar, M. 2018. The effect of ultrasound-assisted vacuum drying on the drying rate and quality of red peppers. Journal of Thermal Analysis and Calorimetry **132**(2), 1131–1143.

Tomsone, L., Kince, T. & Ozola, L. 2018. Effect of drying technologies on bioactive compounds maintenance in pumpkin by-products. *Agronomy Reseach* **16**(4), 1728–1741.

Xie, C., Li, X., Shao, Y. & He, Y. 2014. Color measurement of tea leaves at different drying periods using hyperspectral imaging technique. *PloS One* (61201073), 1–15.

Yagcioglu, A. 1999. Drying characteristic of laurel leaves under different conditions. In Drying Characteristics of Laurel Leaves under Different Conditions. *Proceedings of the 7th International Congress on Agricultural Mechanization and Energy*, Adana, 26-27 May 1999, pp. 565–569.

Younis, M., Abdelkarim, D. & El-abdein, A.Z. 2018. Saudi journal of biological sciences kinetics and mathematical modeling of infrared thin-layer drying of garlic slices. *Saudi Journal of Biological Sciences* **25**(2), 332–338.

Zenoozian, M.S., Devahastin, S., Razavi, M.A., Shahidi, F. & Poreza, H.R. 2014. Use of artificial neural network and image analysis to predict physical properties of osmotically dehydrated pumpkin. *Drying Technology* **26**, 37–41.